

residence time on MMA and DMA sorption to soils is unknown. The long-term incubation of MMA and DMA can cause the biotransformation of As species, and the effect of biotransformation on desorption requires further investigation. It is known that As^V forms inner-sphere complexes, especially bidentate binuclear complexes with ferrihydrite, goethite, gibbsite, and γ -Al₂O₃, and MMA and DMA form bidentate binuclear complexes with amorphous aluminum oxide (AAO).^{2,11–13} MMA and DMA sorption mechanisms to Fe-oxyhydroxides, such as goethite, are not understood well. Investigations on the sorption mechanisms would help to predict the sorption/desorption behavior of MMA and DMA in soils.

Therefore, the objective of this study is to elucidate the soil characteristics that affect MMA and DMA sorption, investigate residence time effects on MMA and DMA desorption, and identify sorption mechanisms between MMA and DMA and goethite. Goethite was chosen as a model Fe-oxyhydroxide due to its presence in soils.

MATERIALS AND METHODS

The details of Materials and Methods are in the Supporting Information.

Materials. Reagent grade As^V, MMA, and DMA were used throughout this study. Goethite was synthesized according to the method described by Schwertmann and Cornell and verified by XRD analysis.¹⁴

The soils that were studied include the topsoil and subsoil of a sandy soil (Fort Mott, Areic Hapludult), a high OM soil (Mullica, Typic Umbraquept), a sandy loam soil (Reybold, Typic Hapludults), and a high Fe containing soil (Cecil, Typic Kanhapludults). The soils were air-dried, ground, passed through a 2 mm sieve, and stored in a refrigerator until experiments were conducted. Soil pH_{water}, organic matter content, and various elemental concentrations were measured, using standard methods (Table S2).

Sorption Isotherm Studies. Sorption isotherms were determined via batch experiments at pH 6 ± 0.1 with various As concentrations, ranging from 50 μM to 2 mM. Soil suspensions (50 g/L) containing 0.01 M NaNO₃ were placed in 50 mL polypropylene centrifuge tubes and equilibrated at pH 6 for 24 h. The pH values of solutions were measured three times daily and were adjusted with 0.1 M HNO₃ or 0.1 M NaOH at pH 6. The suspensions were centrifuged, and supernatants were collected using 0.22 μm pore size Nylon syringe filters. The As concentrations were analyzed using high performance liquid chromatography inductively coupled plasma mass spectrometry (HPLC-ICP-MS).

Sorption Kinetics Studies. Sorption kinetics experiments were conducted using a 50 g/L soil suspension and 0.1 mM MMA or DMA in 0.01 M NaNO₃ at pH 6 with 1 mM 2-(*N*-morpholino)ethanesulfonic acid (MES) buffer. The samples were reacted for various time periods (10 min, 30 min, 1, 2, 6, 12, 24, 48, and 96 h). Suspensions were filtered through 0.22 μm pore size filters. The As concentrations were analyzed using HPLC-ICP-MS.

Desorption Studies. Prior to desorption, 50 g/L soil suspensions were reacted with 0.1 mM MMA or DMA in a 0.01 M NaNO₃ solution at pH 6 for 24 h. After centrifuging, the supernatants were decanted, and the wet soils were saved for the desorption study. The soils were kept in open top bottles covered with aluminum foil to block light and stored in a growth chamber with humidity of 60% for up to 6 months. The water content of the soils was maintained at 75% field capacity. Water

was added, and the soils were mixed and homogenized weekly. After 1 day, 1, 3, and 6 months, small amounts of soils were collected for the desorption experiments. Approximately 1 g of each soil was placed in 50 mL centrifuge tubes and equilibrated with 1 mM phosphate solution, which had a concentration 10× higher than the initial concentrations of MMA or DMA, at pH 6 for 24 h. The tubes were centrifuged, and the supernatants were removed for As speciation analysis. Methylarsenate free 1 mM phosphate solutions were added, and above the process was repeated for 1 week.

X-ray Absorption Spectroscopy (XAS) Investigations. All XAS samples were prepared by reacting 0.1 mM MMA or DMA with 25 g/L goethite suspensions at pH 5 for MMA and pH 6 for DMA samples. After 24 h of reaction, samples were centrifuged and washed with 0.01 M NaNO₃ twice to remove excess As compounds. The wet paste was kept moist by sealing the tubes and analyzed at arsenic K-edge (11,867 eV) at beamline X11A at the National Synchrotron Light Source (NSLS) at Brookhaven National Laboratory, Upton, NY. The SIXPack/IFEFFIT program package was used to analyze the data.¹⁵ Fourier transformation was then performed over the *k*-space range from 2.8 to 10.5 Å⁻¹ for MMA and from 2.8 to 12.5 Å⁻¹ for DMA to obtain the radial distribution functions. Final fitting of the spectra was conducted on Fourier transformed *k*³ weighted spectra in *R* space. The WebAtoms and FEFF7 code were utilized to calculate single scattering theoretical spectra for As–O and As–Fe backscatters using an input file based on the structural refinement of scorodite minerals. During the fitting process, the coordination numbers for MMA and DMA, As–O and As–C, and As–O–O were fixed to reduce adjustable parameters. Only the As–O–O multiple scattering path was included in the fitting, since As–C–O and As–C–C paths had less contributions.

RESULTS AND DISCUSSION

EXAFS Studies. XAS studies on MMA and DMA sorption on the soils were not investigated due to the low sorption on the soils. Instead, MMA and DMA sorption was conducted on goethite, an Fe-bearing mineral and one of the main sorbents of MMA and DMA in the soils (Table S2). Based on the fit for MMA sorbed on goethite, the As–O bond distance was calculated to be 1.70 Å, and the As–C bond distance was 1.89 Å (Table 1). The As–O and As–C bond distances from this study agreed with other experimental studies and XAS investigations.^{2,16,17} MMA sorption resulted in a Fe shell peak appearing in the Fourier transformed *k*³ weighted spectra in *R* space (Figure 1). Approximately 1.8 Fe atoms were located at an As–Fe interatomic distance of 3.31 Å. The coordination number and As–Fe distance were indicative of MMA-goethite bidentate binuclear complexes, which agreed with both MMA-nanocrystalline titanium oxide, MMA-AAO, and As^V-goethite bidentate binuclear complex formation.^{2,10,12,17–19} The previous studies reported the As–Fe interatomic distance to be between 3.23 and 3.37 Å for As–Fe bidentate binuclear complexes. Based on the fit for DMA sorption on goethite, the As–O bond distance was calculated to be 1.71 Å, while the As–C bond distance was 1.91 Å (Table 1). The As–O and As–C bond distances from this study agreed with other experimental studies and XAS investigations.^{2,16,17} DMA sorption also resulted in a Fe shell peak (Figure 1) with 1.9 Fe atoms located at an As–Fe interatomic distance of 3.30 Å. The coordination number and As–Fe distance were indicative of DMA-goethite bidentate binuclear complexes, which is consistent with published EXAFS

Table 1. Structural Parameters for XAS Analysis of MMA and DMA Sorbed on Goethite

		MMA-Fe	DMA-Fe	As ^V -Fe ^s
As-O	CN ^a (Fixed)	3	2	
	R ^b (Å)	1.70 ± 0.008 ^f	1.71 ± 0.0056	
	σ ^{2c} (Å ²)	0.0010 ± 0.0007	0.0011 ± 0.0005	
As-C	CN (Fixed)	1	2	
	R (Å)	1.89 ± 0.01	1.91 ± 0.009	
	σ ² (Å ²)	0.001 ± 0.001	0.0009 ± 0.0004	
As-O-O	CN (Fixed)	6	2	
	R (Å)	3.12 ± 0.05	3.15 ± 0.02	
	σ ² (Å ²)	0.0069 ± 0.004	0.0070 ± 0.003	
As-Fe	CN	1.8 ± 1.1	1.9 ± 0.5	1.3-2.9
	R (Å)	3.31 ± 0.03	3.30 ± 0.08	3.23-3.37
	σ ² (Å ²)	0.008 ± 0.002	0.0069 ± 0.0008	0.0028-0.01
	E ₀ ^d (eV)	4.13 ± 0.9	4.30 ± 0.86	
	S ₀ ^{2e} (Fixed)	0.98	0.98	

^a Coordination number. ^b Interatomic distance. ^c Debye-Waller factor. ^d Energy shift. ^e Amplitude reduction factor. ^f Standard deviation. ^g Selected references of As^V sorbed on goethite analyzed by EXAFS.^{10,12,18,19}

studies and density functional theory (DFT) studies, reporting As-Fe bidentate binuclear complex formation.^{12,19}

It has been reported that DMA forms monodentate mononuclear complexes with nanocrystalline titanium oxide and bidentate binuclear complexes with AAO.^{2,17} The difference in the type of DMA surface complexes could be due to differences in experimental conditions and the surface charge of titanium oxide and Fe-oxyhydroxide.² The As-Fe interatomic distance of 3.30 Å is too close for As-Fe monodentate mononuclear complexes, which is 3.6 Å based on EXAFS studies and 3.67 Å based on DFT calculations.^{12,19} The coordination numbers of As-Fe themselves cannot be conclusive due to the large standard deviation. Considering both interatomic distance and coordination number, we conclude that DMA forms bidentate binuclear complexes with goethite. Although we report inner-sphere complex formation between MMA/DMA and goethite, it is not the only MMA and DMA sorption mechanism on goethite. It is likely that MMA and DMA also simultaneously form outer-sphere complexes based on other studies.^{20,21} The As-Fe interatomic distance in outer-sphere complexes is greater than 5 Å.²¹ With the long interatomic distances, the As-Fe scattering becomes extremely weak, and the variation in the interatomic distance increases the Debye-Waller factor to an extremely large value such that the As-Fe peak observed in Fourier transformed spectra is not intense enough to be fit. The EXAFS spectroscopy technique is not suitable for studying the longer interatomic distances of outer-sphere complexes. In situ resonance X-ray scattering and Fourier transform infrared spectroscopy (FTIR) studies were able to identify the outer-sphere complex formation between As^V and hematite and DMA and goethite/hematite.^{20,21} The resonance X-ray scattering study was able to locate As atoms as far as 2.9 Å above the terminal oxygen atoms of the hematite surface, forming outer-sphere complexes. The FTIR study observed peak changes due to outer-sphere complex formation between DMA and goethite. Since the molecular structure of MMA and sorption behavior of MMA toward goethite/hematite are comparable to As^V and DMA, it is possible that MMA also forms outer-sphere complexes with goethite.

Sorption Isotherms. Sorption isotherms for MMA and DMA exhibited L-shaped (Langmuir) type isotherms (Figure 2).²² The sorption percentage decreased as initial As concentration increased, because available sorption sites decrease as the sites are occupied by

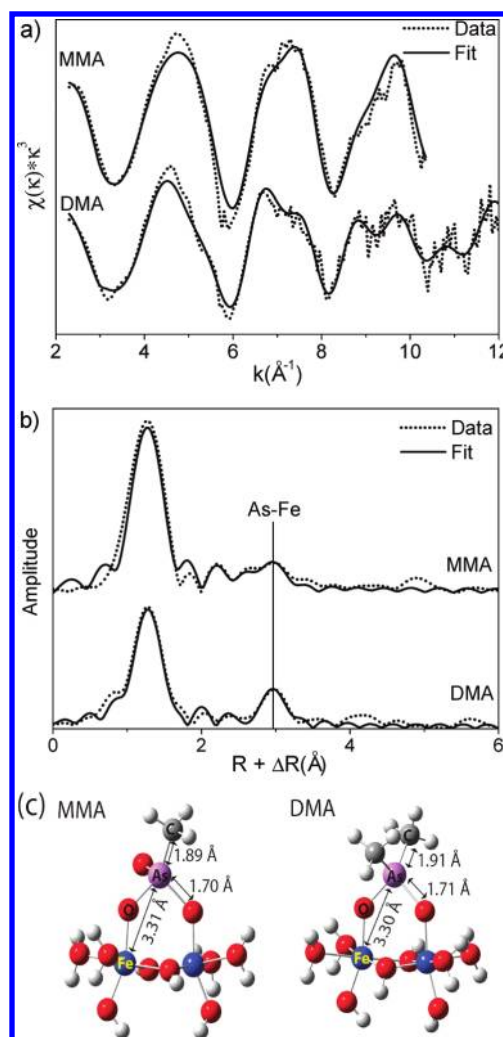


Figure 1. MMA and DMA XAS spectra in (a) k space, (b) Fourier transformation of XAS spectra, and (c) molecular configurations of MMA and DMA sorbed on goethite cluster created by GaussView.³⁶

more MMA or DMA. For both MMA and DMA sorption samples, the highest sorption occurred in the Cecil subsoil, which contained the highest amount of Al/Fe-oxyhydroxides (Table S2). Sorption maxima, based on the Langmuir equation, were also the highest for the Cecil subsoil (Table S3). At the initial MMA or DMA concentrations of 2 mM, the overall order of the highest MMA and DMA sorption on the soils was as follows: Cecil subsoil > Reybold subsoil > Cecil topsoil > Mullica topsoil. The sorption capacity order was approximately proportional to the Al/Fe-oxyhydroxide concentration in the soils (Figure S3) with R^2 values between CBD extracted Fe content and MMA/DMA sorption of 0.66 and 0.74, respectively. Such correlation is consistent with other studies.^{2,11,23-25} MMA and DMA sorption to other soil components, such as clay minerals or quartz, is likely not as significant as Al/Fe-oxyhydroxides, based on As^V sorption to these minerals.^{26,27} In fact, the Fort Mott soils with the highest sand content sorbed the least amounts of both MMA and DMA.

Possible sorption mechanisms between MMA or DMA and Al/Fe-oxyhydroxides are inner-sphere complexes and outer-sphere complexes. In this study, we consider that inner-sphere complexes are due to ligand exchange and MMA and DMA are directly bound to the surface and outer-sphere complexes are due

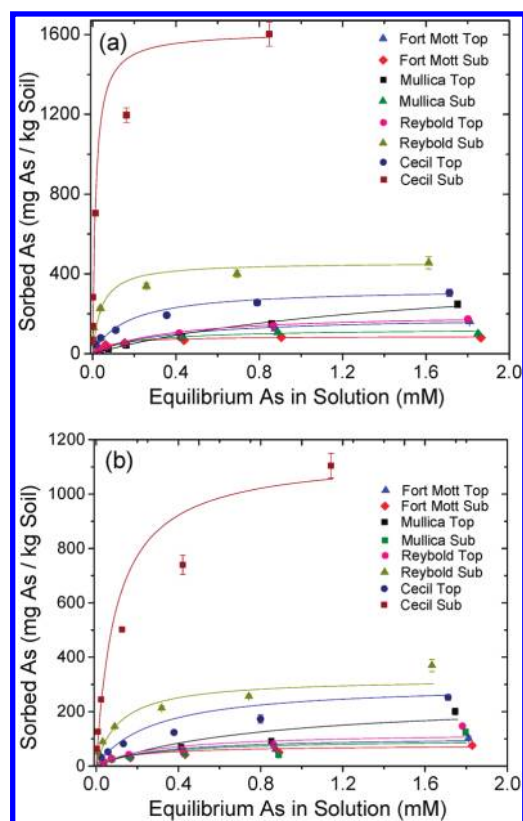


Figure 2. Sorption isotherm studies. a) MMA sorption to soils and b) DMA sorption to soils. Lines are based on fitted Langmuir equation.

to electrostatic interactions or hydrogen bonding to the surface and MMA and DMA are not directly bound to the surface. Inner-sphere complex formation has been discussed above. Outer-sphere complexes can be formed between negatively charged MMA/DMA and the positively charged Al/Fe-oxide surface. At pH 6, the dominant MMA ($pK_{a1} = 4.2$) species was $\text{CH}_3\text{HAsO}_3^-$, and similar amounts of both DMA ($pK_a = 6.1$) species, $(\text{CH}_3)_2\text{HAsO}_2$ and $(\text{CH}_3)_2\text{AsO}_2^-$, existed (Table S1). The Al/Fe-oxyhydroxide surface is positively charged at pH 6, since the PZC values of these oxyhydroxides are often above pH 8.^{2,11,25,28} Thus, the experimental conditions in this study would promote outer-sphere complex formation of MMA or DMA with the Al/Fe-oxyhydroxide surface. At pH 6, other soil constituents, such as clays, are likely negatively charged based on their PZC values, which are between 2 and 4.²² Negatively charged As species are less likely to sorb on negatively charged clays. The main sorbents in our study are likely Al/Fe oxyhydroxides.

Sorption Kinetics Studies. The sorption kinetics experiments revealed biphasic sorption characteristics: fast initial sorption followed by slow continuous sorption (Figure 3), similar to other As sorption kinetics studies.^{2,29,30} The possible slow continuous sorption could be attributed to diffusion into the interiors of aggregates or different sites of reactivity.^{10,29}

The MMA and DMA sorption rates are also approximately proportional to the Al/Fe concentration in the soils (Table S4). The first order kinetics model was applied, and initial rate constants were estimated (Table S4). Among MMA sorption samples, the Cecil subsoil had the fastest sorption rate. Almost 100% (of the initial MMA added) was sorbed within 1 h of reaction. Initial MMA sorption on the Reybold subsoil was only 70% of

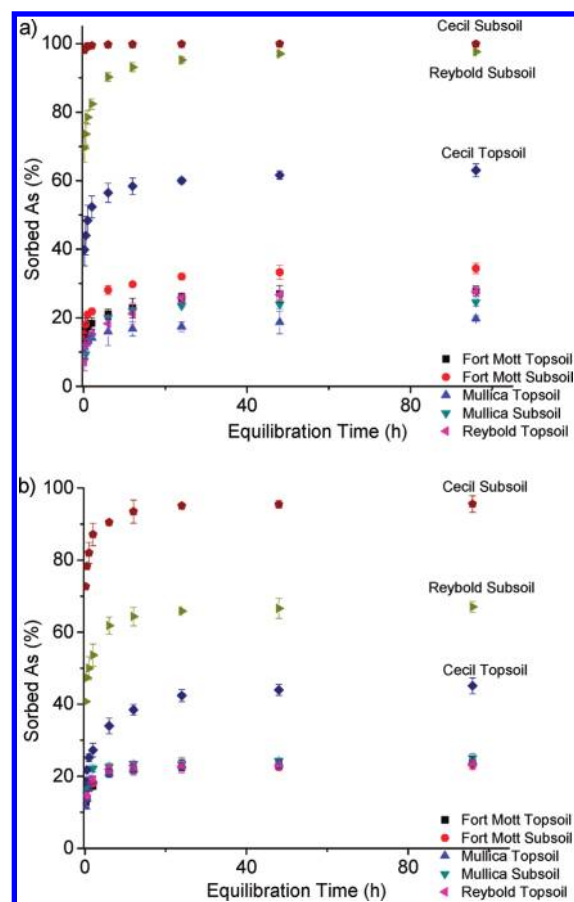


Figure 3. MMA (a) and DMA (b) sorption kinetics.

initial MMA, but by the end of the 96 h reaction period, total sorption was close to what was observed for the Cecil subsoil. The third highest amount of MMA sorption was observed for the Cecil topsoil with 63% sorption. The other soils had similar amounts of MMA sorption ranging from 20 to 34% of initially added MMA (Figure 3). DMA sorption on these soils showed a similar trend, but the sorption capacity was lower than MMA sorption, the Cecil subsoil sorbing 95% of initially added DMA, the Reybold subsoil sorbing 67%, and the Cecil topsoil sorbing 45%. The remaining five soils had around 25% sorption at 96 h. For the Cecil subsoil, the Reybold subsoil, and the Cecil topsoil, the rapid sorption continued for the first 24 h. For the other five soils, the rapid sorption continued for only the first 6 h.

MMA sorption was consistently higher than DMA sorption in both the isotherm and kinetics studies, similar to MMA and DMA sorption to ferrihydrite, goethite, and AAO.^{2,25} The main cause of lower sorption for DMA is possibly due to the additional methyl group substitution.^{2,25} The additional methyl group eliminates a deprotonation site from DMA so that DMA is less negatively charged at any given pH, which leads to less electrostatic attraction. Less electrostatic attraction can affect the amount of outer-sphere complex formation.^{21,31} Additional methyl groups also make the DMA molecule larger, occupying more space per molecule. Less hydrogen bonding is formed with the oxide surface oxy/hydroxyl groups. Thus, fewer potential As binding sites are available for inner- and outer-sphere complex formation.

The Effect of Organic Matter on Sorption. Organic matter is generally a negatively charged component and can interact with

positively charged Al/Fe-oxyhydroxides at pH 6. OM can sorb to Al/Fe-oxyhydroxides and compete with As for the same binding sites, resulting in less As sorption to the oxyhydroxides.³² In addition, the sorption of OM on Al/Fe-oxyhydroxides lowers the PZC of the oxyhydroxides,³³ causing the Al/Fe oxyhydroxide surfaces to be less positively charged, which results in less electrostatic attraction and, therefore, less sorption. The Mullica topsoil, which had the highest OM % of the soils, sorbed the least amount of MMA and DMA at lower initial MMA and DMA concentrations (Figure 2). The Mullica topsoil had the second lowest Fe-oxyhydroxide concentration but had over 1000 mg/kg Al-oxyhydroxides (Table S2), which was higher than the other soils that had higher MMA and DMA sorption than the Mullica topsoil. It is possible that MMA and DMA competed for the same binding sites with OM in the Mullica topsoil, and many available binding sites were preoccupied by OM, resulting in lower MMA and DMA sorption to the Mullica topsoil. However, a clear correlation between OM % and MMA and DMA sorption was not observed among the soils (Figure S3). In addition, the sorption data were plotted against OM % divided by total Fe-oxyhydroxide (OM %/total Fe-oxyhydroxides), but a clear linear correlation was not observed (data not shown). It is possible that the effect of Fe-oxyhydroxides on MMA and DMA sorption is much greater than OM, which masks a correlation between OM and MMA and DMA sorption. Further sorption studies on more soils with various OM % would be required to determine the effect of OM on MMA and DMA sorption.

Desorption. Results from the desorption of MMA and DMA reacted samples (MMA samples and DMA samples) varied from soil to soil (Figure 4), and no significant correlations between the amount of desorption and specific soil characteristics, such as Al/Fe-oxyhydroxide concentrations or OM % in the soils, were observed. As^V and DMA were produced as a result of methylation and demethylation of MMA or DMA by microbes, which likely occurred during the soil incubation,¹ which agreed with other studies where initially applied MMA and DMA were demethylated to inorganic As species.^{4,5,8,34} In a separate study, most of the sorbed As species was As^V when the Reybold subsoil was incubated for 1 year under different incubation conditions.⁴

In MMA samples, after 1 day of sorption, 64–84% of sorbed MMA was desorbed, and all of the desorbed As was MMA (Figure 4, S4). The total desorbed As, the sum of desorbed MMA, DMA, and As^V, decreased over time. After 6 months of residence time, 42–77% of sorbed As was desorbed. The Cecil subsoil had the highest As retention. After 1 day of sorption, 65% of sorbed MMA was desorbed. The percentage finally dropped to 42% after 6 months of incubation. In DMA samples, the average As desorption was higher than for the MMA samples. After 1 day of sorption, 73–88% of sorbed DMA was desorbed (Figure S4). The total desorbed As, the sum of desorbed MMA, DMA, and As^V, also decreased over time. Among the soil samples, the Fort Mott topsoil retained the highest amount of As (Figure 4). After 1 day of sorption, 77% of the sorbed DMA was desorbed. The desorption percentage dropped to 56% after 6 months incubation.

There are several possible explanations for decreasing total As desorption with longer residence times. MMA and DMA desorption is often limited by diffusion processes.²⁹ At the fast initial MMA and DMA sorption phase, they can be sorbed on the exterior of mineral particles, which can be accessible over short times. At longer reaction times, MMA and DMA diffuse into the interior of particles and micropores. The MMA and DMA from the interiors of particles have to diffuse out to be desorbed.

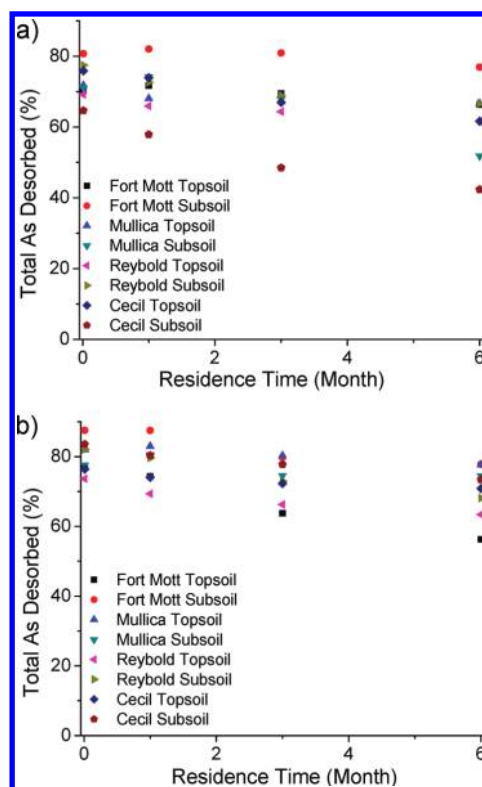


Figure 4. MMA and DMA desorption as affected by residence time a) total As desorption (the sum of MMA, As^V, and DMA) from MMA reacted samples and b) total As desorption (the sum of DMA and As^V) from DMA reacted samples.

In theory, if the diffusion into the interior of particles takes a month, the diffusion from the interior of particles requires the same amount of time. Soils are heterogeneous systems that consist of networks of macro- and micropore/particles that promote diffusion processes. Thus, 1 week might not be long enough to desorb part of the MMA and DMA, and they would remain in the soils.

Another possible explanation for the less desorption at longer residence times could be due to a transformation in sorption complexation.⁹ Over time, MMA or DMA sorbed via electrostatic attraction or outer-sphere complexes may transform to inner-sphere complexes, causing the MMA and DMA to be more difficult to desorb.

Also, the formation of stable surface precipitate/sorption complexes is possible as observed in other studies.⁹ Even though our systems had a water content of 75% field capacity, a part of the Al/Fe-oxyhydroxide surface can be dissolved at the mineral/water interface. When both MMA and DMA form bidentate binuclear complexes with Fe-oxyhydroxides (Figure 1), MMA still has an oxy/hydroxyl group that is not involved in complex formation. The oxygen atoms in the oxy/hydroxyl group have lone pairs of electron that make the functional group relatively negatively charged and can electrostatically attract positively charged Al/Fe ions, while DMA has only two methyl groups not involved in complex formation. Methyl groups are neutral functional groups and cannot electrostatically attract Al/Fe ions. The decrease in As desorption in the MMA reacted Cecil subsoil is much larger than the DMA reacted Cecil subsoil, which could be due to surface precipitate formation.

Another possible explanation for less desorption at longer residence times is due to the increasing sorption of As^V. A portion of sorbed MMA and DMA is demethylated to As^V, and the As^V is sorbed on the soils. Microfocused XANES analysis of sorbed As on the Reybold subsoil identified an increasing peak that corresponded to As^V as sample incubation time increased up to 1 year.⁴ The same situation can be applied to this study. Subsequently, the sorbed As^V was desorbed by phosphate (Figure S4), which confirmed the demethylation and sorption. The demethylation increases over time, and more As^V is produced and sorbed to the soils. Although irreversible sorption behaviors are observed for As^V, MMA, and DMA, the As^V retention is the highest so that As^V is not desorbed as easily as MMA and DMA even though phosphate was applied for a week, resulting in decreases in the amount of desorption.^{2,25} No As^V was desorbed from the 1 day samples, but desorbed As^V ranged from less than 1% to 14% of sorbed MMA and 1.5% to 39% of sorbed DMA for the six month samples.

The irreversible sorption was observed even when the residence time was only 1 day (Figure 4). As the EXAFS studies (Figure 1) suggest, the irreversible sorption is likely due to inner-sphere complex formation, which often causes irreversible processes.²² The differences in desorption amounts between MMA and DMA are likely due to the DMA bidentate binuclear complex being not as strong as the MMA bidentate binuclear complex, and the complex formation can be reversible to some extent.² Another possibility is that MMA and DMA simultaneously form both inner and outer-sphere complexes, and the ratio of inner-sphere complexes to outer-sphere complexes is different. DMA could form a larger proportion of outer-sphere complexes than As^V or MMA does, which can be easily desorbed. Further sorption mechanism studies, such as resonance anomalous X-ray reflectivity measurements, can help to verify such speculation.

The effect of OM on demethylation is not clear. Topsoils have higher rates of demethylation and higher OM % compared to corresponding subsoils (Figure 4 and Table S2). The OM can be enhancing microbial activity, but studies have shown that the addition of cellulose or carbohydrates actually retard the methylation/demethylation rate.^{34,35} A clear conclusion on the effect of OM cannot be made, but it is possible that microbial community diversity could affect the degree of demethylation. Also, in the soil samples, the higher degree of DMA demethylation over MMA demethylation is consistent with other studies and is likely due to the weaker sorption affinity for DMA that can promote more demethylation by microbes.³⁴

Environmental Significance. A better understanding of MMA and DMA sorption/desorption is critical to predict the fate of these chemicals in the environment. Our study revealed that MMA and DMA are mainly sorbed to Al/Fe-oxyhydroxides in soils, and the sorption rate and capacity depends on the quantity of Fe and Al. A part of the irreversible MMA and DMA sorption is due to the strong inner-sphere bidentate binuclear complex formation between MMA and DMA and the goethite surface, similar to As^V sorption on goethite. The decreasing desorption of MMA and DMA over time suggests a possible accumulation of As as either organic or inorganic species during long-term agricultural applications. When these fields are used for agricultural production, the uptake of As by plants is possible. Accordingly, MMA and DMA sorption/desorption and biotransformation can play an important role in total arsenic cycling in the environment. Understanding MMA and DMA sorption mechanisms are also useful for establishing important parameters for surface complexation model development.

■ ASSOCIATED CONTENT

S Supporting Information. Detailed Materials and Methods sections and additional figures and tables. This material is available free of charge via the Internet at <http://pubs.acs.org>.

■ AUTHOR INFORMATION

Corresponding Author

*Phone: (302)831-1286. E-mail: mshimizu@udel.edu.

■ ACKNOWLEDGMENT

We would like to thank Dr. John Galbraith from Virginia Polytechnic Institute and State University and Mr. Phillip King from the United States Department of Agriculture Natural Resources Conservation Service for assisting in soil sampling. Portions of this work were performed at Beamline X11A, NSLS, Brookhaven National Laboratory. Beamline X11A is supported by the Office of Naval Research and contributions from Participating Research Team (PRT) members. Use of the NSLS was supported by DOE under Contract No. DE-AC02-98CH10886.

■ REFERENCES

- (1) Cullen, W. R.; Reimer, K. J. Arsenic speciation in the environment. *Chem. Rev.* **1989**, *89* (4), 713–764.
- (2) Shimizu, M.; Ginder-Vogel, M.; Parikh, S. J.; Sparks, D. L. Molecular scale assessment of methylarsenic sorption on aluminum oxide. *Environ. Sci. Technol.* **2010**, *44* (2), 612–617.
- (3) Sohrin, Y.; Matsui, M.; Kawashima, M.; Hojo, M.; Hasegawa, H. Arsenic biogeochemistry affected by eutrophication in Lake Biwa, Japan. *Environ. Sci. Technol.* **1997**, *31* (10), 2712–2720.
- (4) Shimizu, M.; Arai, Y.; Sparks, D. L. Multi-scale Assessment of Methylarsenic Reactivity in Soil: 2. Distribution and Speciation in Soil. *Environ. Sci. Technol.* **2011**, *45*, 4300–4306.
- (5) Woolson, E. A.; Aharonson, N.; Iadevaia, R. Application of the high-performance liquid-chromatography flameless atomic-absorption method to the study of alkyl arsenical herbicide metabolism in soil. *J. Agric. Food Chem.* **1982**, *30* (3), 580–584.
- (6) Dickens, R.; Hiltbold, A. E. Movement and persistence of methanearsonates in soil. *Weeds* **1967**, *15* (4), 299–304.
- (7) Wauchope, R. D. Fixation of arsenical herbicides, phosphate, and arsenate in alluvial soils. *J. Environ. Qual.* **1975**, *4* (3), 355–358.
- (8) Bednar, A. J.; Garbarino, J. R.; Ranville, J. F.; Wildeman, T. R. Presence of organoarsenicals used in cotton production in agricultural water and soil of the southern United States. *J. Agric. Food Chem.* **2002**, *50* (25), 7340–7344.
- (9) Arai, Y.; Sparks, D. L. Residence time effects on arsenate surface speciation at the aluminum oxide-water interface. *Soil Sci.* **2002**, *167* (5), 303–314.
- (10) O'Reilly, S. E.; Strawn, D. G.; Sparks, D. L. Residence time effects on arsenate adsorption/desorption mechanisms on goethite. *Soil Sci. Soc. Am. J.* **2001**, *65* (1), 67–77.
- (11) Arai, Y.; Elzinga, E. J.; Sparks, D. L. X-ray absorption spectroscopic investigation of arsenite and arsenate adsorption at the aluminum oxide-water interface. *J. Colloid Interface Sci.* **2001**, *235* (1), 80–88.
- (12) Fendorf, S.; Eick, M. J.; Grossl, P.; Sparks, D. L. Arsenate and chromate retention mechanisms on goethite 0.1. Surface structure. *Environ. Sci. Technol.* **1997**, *31* (2), 315–320.
- (13) Ladeira, A. C. Q.; Ciminelli, V. S. T.; Duarte, H. A.; Alves, M. C. M.; Ramos, A. Y. Mechanism of anion retention from EXAFS and density functional calculations: Arsenic (V) adsorbed on gibbsite. *Geochim. Cosmochim. Acta* **2001**, *65* (8), 1211–1217.
- (14) Schwertmann, U.; Cornell, R. M. *Iron oxides in the laboratory*; VCH: Weinheim, 1991.

- (15) Webb, S. M. SIXpack: A graphical user interface for XAS analysis using IFEFFIT. *Phys. Scr., T* **2005**, *T115*, 1011–1014.
- (16) Grundler, H. V.; Schumann, H. D.; Steger, E. Raman and infrared spectroscopic investigation of alkyl derivatives of arsenic acid 0.6. AsO bond - calculation of force constants and vibrational energy-distribution in compounds of type $RAsO_3X_2$ and R_2AsO_2X . *J. Mol. Struct.* **1974**, *21* (1), 149–157.
- (17) Jing, C. Y.; Meng, X. G.; Liu, S. Q.; Baidas, S.; Patraju, R.; Christodoulatos, C.; Korfiatis, G. P. Surface complexation of organic arsenic on nanocrystalline titanium oxide. *J. Colloid Interface Sci.* **2005**, *290* (1), 14–21.
- (18) Foster, A. L.; Brown, G. E.; Tingle, T. N.; Parks, G. A. Quantitative arsenic speciation in mine tailings using X-ray absorption spectroscopy. *Am. Mineral.* **1998**, *83* (5–6), 553–568.
- (19) Sherman, D. M.; Randall, S. R. Surface complexation of arsenic(V) to iron(III) (hydr)oxides: Structural mechanism from ab initio molecular geometries and EXAFS spectroscopy. *Geochim. Cosmochim. Acta* **2003**, *67* (22), 4223–4230.
- (20) Adamescu, A.; Mitchell, W.; Hamilton, I. P.; Al-Abadleh, H. A. Insights into the surface complexation of dimethylarsinic acid on iron (oxyhydr)oxides from ATR-FTIR studies and quantum chemical calculations. *Environ. Sci. Technol.* **2010**, *44* (20), 7802–7807.
- (21) Catalano, J. G.; Park, C.; Fenter, P.; Zhang, Z. Simultaneous inner- and outer-sphere arsenate adsorption on corundum and hematite. *Geochim. Cosmochim. Acta* **2008**, *72* (8), 1986–2004.
- (22) Sparks, D. L. *Environmental Soil Chemistry*, 2nd ed.; Academic Press: Boston, 2002.
- (23) Jain, A.; Raven, K. P.; Loeppert, R. H. Arsenite and arsenate adsorption on ferrihydrite: Surface charge reduction and net OH⁻ release stoichiometry. *Environ. Sci. Technol.* **1999**, *33* (8), 1179–1184.
- (24) Woolson, E. A. Persistence and chemical distribution of arsenic acid in three soils. *J. Agric. Food Chem.* **1975**, *23* (4), 677–681.
- (25) Lafferty, B. J.; Loeppert, R. H. Methyl arsenic adsorption and desorption behavior on iron oxides. *Environ. Sci. Technol.* **2005**, *39* (7), 2120–2127.
- (26) Ladeira, A. C. Q.; Ciminelli, V. S. T. Adsorption and desorption of arsenic on an oxisol and its constituents. *Water Res.* **2004**, *38* (8), 2087–2094.
- (27) Manning, B. A.; Goldberg, S. Modeling arsenate competitive adsorption on kaolinite, montmorillonite and Illite. *Clays Clay Miner.* **1996**, *44* (5), 609–623.
- (28) Shibata, J.; Fuerstenau, D. W. Flocculation and flotation characteristics of fine hematite with sodium oleate. *Int. J. Miner. Process* **2003**, *72* (1–4), 25–32.
- (29) Fuller, C. C.; Davis, J. A.; Waychunas, G. A. Surface-Chemistry of Ferrihydrite 0.2. Kinetics of Arsenate Adsorption and Coprecipitation. *Geochim. Cosmochim. Acta* **1993**, *57* (10), 2271–2282.
- (30) Raven, K. P.; Jain, A.; Loeppert, R. H. Arsenite and arsenate adsorption on ferrihydrite: Kinetics, equilibrium, and adsorption envelopes. *Environ. Sci. Technol.* **1998**, *32* (3), 344–349.
- (31) Sposito, G. The operational definition of the zero-point of charge in soils. *Soil Sci. Soc. Am. J.* **1981**, *45* (2), 292–297.
- (32) Redman, A. D.; Macalady, D. L.; Ahmann, D. Natural organic matter affects arsenic speciation and sorption onto hematite. *Environ. Sci. Technol.* **2002**, *36* (13), 2889–96.
- (33) Harter, R. D.; Naidu, R. Role of metal-organic complexation in metal sorption by soils. In *Advances in Agronomy, Vol 55*; Academic Press Inc.: San Diego, 1995; Vol. 55, pp 219–263.
- (34) Gao, S.; Burau, R. G. Environmental factors affecting rates of arsine evolution from and mineralization of arsenicals in soil. *J. Environ. Qual.* **1997**, *26* (3), 753–763.
- (35) Huysmans, K. D.; Frankenberger, W. T. Evolution of trimethylarsine by a *Penicillium* Sp isolated from agricultural evaporation pond water. *Sci. Total Environ.* **1991**, *105*, 13–28.
- (36) Dennington, R., II; Keith, T.; Millam, J.; Eppinnett, K.; Hovell, W. L.; Gilliland, R. *GaussView, Version 3.09*; Semichem, Inc.: Shawnee Mission, KS, 2003.